Potential *Adenostemma lavenia* and *Muntingia calabura* Extracts to Inhibit Cyclooxygenase-2 Activity as a Therapeutic Strategy for Anti-inflammation: Experimental and Theoretical Studies

Bagaskoro Tuwalaid[1], Dyah Iswantini[1,2], and Setyanto Tri Wahyudi[3*]

[1]*Department of Chemistry, Faculty of Mathematics and Natural Sciences, IPB University, Bogor 16680, Indonesia*

[2]*Tropical Biopharmaca Research Center, IPB University, Taman Kencana Campus, Bogor 16128, Indonesia*

[3]*Department of Physics, Faculty of Mathematics and Natural Sciences, IPB University, Bogor 16680, Indonesia*

**** Corresponding author:***

email: stwahyudi@apps.ipb.ac.id

Received: November 28, 2021
Accepted: February 18, 2022

DOI: 10.22146/ijc.70794

Abstract: *Continuous inflammation can cause new and more severe diseases, thus effective treatments are needed. One of the common inflammation treatments is given by reducing prostaglandins' production through the inhibition of COX-2 activity. This experiment aims to examine the potential application of plant extracts of* Adenostemma lavenia *and* Muntingia calabura *(Jamaica cherry) as anti-inflammatory agents in inhibiting COX-2 activity through* in silico *and* in vitro *assays. Molecular docking and molecular dynamics simulation were accomplished to evaluate the stability of the complex between COX-2 and ligands. The COX-2 inhibition was determined using the COX-2 Inhibitor Screening Assay KIT. Based on the docking results, the active compound from* A. lavenia*, ligand 1a,9b-dihydro-1H-cyclopropa[a]anthracene, has the lowest binding energy of -8.7 kcal/mol. In comparison,* M. calabura *contains 7-hydroxyflavone ligand with a Gibbs free energy of -9.1 kcal/mol. The molecular dynamics study demonstrates that COX-2 maintains its stability when forming interactions with selected compounds from all the tested extracts. The results of the COX-2 inhibition test showed that 96% EtOH extract of* A. Lavenia *at concentrations of 25 and 100 ppm had an inhibitory activity of 98%; meanwhile, 70% and 96% EtOH extracts of* M. calabura *at 1000 ppm concentration could inhibit COX-2 activity up to 100%. The results demonstrate that both plants show potential anti-inflammatory activity.*

Keywords: *anti-inflammatory; herbal medicine;* in vitro*; molecular docking; molecular dynamics*

■ INTRODUCTION

Inflammation is a biological response of the immune system triggered by some factors, such as exogenous substances, pathogens, damaged cells, and toxic compounds that enter the body. These factors can cause acute or chronic inflammatory responses in the body that may end up in serious diseases such as rheumatoid arthritis, lung, cancer, and heart disease [1]. Inflammation is usually suffered by patients infected with Covid-19. Several studies concluded that the hyperinflammatory response of SARS-CoV-2 is a significant cause of illness severity and death in infected patients [2]. Furthermore, continuous inflammation can cause new problems in the area where inflammation occurs and can trigger the proliferation of cancer cells. Therefore, prevention and treatment efforts to reduce inflammation in the body are needed [3].

Inflammation is usually triggered by several inflammatory mediators, one of which is prostaglandins. Prostaglandins are produced from arachidonic acid metabolism catalyzed by the COX-2 enzyme. Therefore, one of the efforts to prevent inflammation is to inhibit COX-2 activity [4]. The drugs that can inhibit COX-2 activity are classified as non-steroidal anti-inflammatory drugs. Non-steroidal anti-inflammatory drugs are one of

the generally prescribed ache medications. Unfortunately, long-term use can cause more harmful side effects such as gastrointestinal bleeding, cardiovascular side effects, and nephrotoxicity [5]. Therefore, it is preferable to use drugs derived from natural products to minimize the side effects. Searching for drug compounds that can inhibit COX-2 can be carried out using the molecular docking method and continued with molecular dynamics studies.

Molecular docking is a process in which small molecules are anchored into macromolecular structures such as proteins, polysaccharides, carbohydrates, and double-helical DNA structures to assess their complementary value at the binding site [6]. The molecular docking technique aims to predict the most suitable binding mode of the ligand to the receptor. This method can estimate the binding affinity between the ligand and protein and the protein-ligand complex structure [7]. Receptors in molecular docking can be assumed to be rigid molecules (immobile) and might also be considered flexible molecules similar to their natural state [8]. The stability of receptor binding with ligands resulting from the docking process can be calculated using molecular dynamics simulations. Molecular dynamics (MD) is a computational physics method to study and analyze the interactions and movements of atoms and molecules based on Newton's laws. The force field is used to estimate the forces between the interacting particles and calculate the system's total energy consisting of bond energy, angular energy, dihedral energy, electrostatic energy, and van der Waals energy [9]. MD is commonly carried out using the AMBER20 program because this program is non-periodic simulations, the use of a generalized Born or numerical Poisson-Boltzmann implicit solvent model, free-energy calculations use thermodynamic integration, and there may be widespread assistance for trajectory evaluation and active post-processing [10]. The root means square deviation (RMSD), a radius of gyration residue (Rg), the root means square fluctuation (RMSF), and the total energy of the molecular dynamics simulation path are the basic parameters to measure the stability of a system.

Anti-inflammatory drugs circulating in public tend to have dangerous side effects, so an alternative that can be used is by utilizing herbal medicines derived from plants. The use of herbal medicines is expected to contain safe therapeutic compounds, the resulting side effects are not destructive, and the treatment of inflammation is more effective. The plants that would have been tested for anti-inflammatory activity as herbal medicine in this study are *Adenostemma lavenia* (sticky daisy, *legetan warak*) and *Muntingia calabura (Jamaica cherry, kersen).* Compounds in the ethanolic extract of *A. lavenia* have been reported to inhibit COX-2 activity [11]. The active compound in the root is 11-hydroxylated kauranic acids, which are beneficial as an anti-inflammatory, improve lung and liver function, and relieve pain [12]. Increasing the concentration of *M. calabura* fruit extract has been known to reduce prostaglandins concentration in the body [13]. This study was designed to examine the potential of these two plants as anti-inflammatory agents in inhibiting COX-2 activity through *in silico* and *in vitro* experiments.

■ EXPERIMENTAL SECTION

Materials

The material used for the *in silico* test is a 3D structure of COX-2 protein with the PDB code 5IKR. The ligands used were 49 compounds in *A. lavenia*, and 68 compounds in *M. calabura*. Materials for *in vitro* tests were 50%, 70%, and 96% ethanol extracts from leaves of the respective species, provided by the Tropical Biopharmaca Research Center Laboratory, Bogor City, Indonesia.

Procedure

Preparation of molecular docking

The receptor used is the human co-crystal structure of the COX-2 protein with the PDB code 5KIR. The 3D structure is obtained from the Protein Data Bank (PDB) database in a *.pdb file on www.rcsb.org. The 3D structure of the COX-2 protein was then examined for completeness of the residue using the UCSF-Chimera software [14]. The last preparation was removing the ligands and water present in the receptor and adding Gasteiger charge and polar hydrogen using AutodockTools 1.5.6.rc3 [15]. The ligands were 49

compounds in *A. Lavenia* leaves, and 68 compounds in *M. calabura* leaves based on literature studies (Suppl. 1 and 2), encompassing polar and semipolar compounds. The 3D structures of the compounds were obtained from the https://pubchem.ncbi.nlm.nih.gov/. Each ligand structure was optimized using quantum mechanics (QM) calculations using the xTB program. Finally, each compound was charged, and the torque was adjusted using AutodockTools 1.5.6.rc3 software. The ligands that gave the most negative Gibbs free energy value were determined by their physicochemical properties using Lipinski's rule.

Running and evaluation of molecular docking

The grid box was determined based on the shape of a protein with the appropriate X, Y, and Z-axis values. The grid box parameters used for each process are shown in Table 1. Next, the target protein and ligand docking simulation were performed in *.pdbqt format. Molecular docking was processed using Autodock Vina software with an exhaustiveness value of 8. Each ligand was flexible and would interact with the receptor in strict conditions. Afterward, a docked output ligand structure file (out. pdbqt) and a text file (log.txt) appeared containing data on the energy value of the affinity of the ligand to the receptor for each ligand conformational mode. The final step was assessing the molecular docking results using the DS visualizer software. The hydrogen bonds and the contact residues between ligands and target protein were observed using DS visualizer software with *.pdb format [16]. Finally, with the lowest Gibbs free energy (ΔG), the docked ligand compounds were tested for toxicity using Data Warrior software.

Molecular dynamics simulation and evaluation of the results

Molecular dynamics simulations were carried out on COX-2 protein and the five best ligands based on molecular docking results. Each complex molecule was provided with a folder for running molecular dynamics simulations. Before running the simulation, the proteins and the ligands were prepared. The ligands and the target proteins were combined to form protein-ligand complexes using AutodockTools. The complexes were then processed using the Pdb4amber program to remove water and hydrogen molecules. Next, the hydrogens were added to the complex and neutralized the pH to 7 using a webserver (http://biophysics.cs.vt.edu/H++) [17-19]. The results of the H++ webserver were in the form of topology files and coordinates. Next, the protein and the ligand files were combined to form a ligand-protein complex PDB file parameterized by tLEaP using the Amber FF14SB and GAFF2 force field for proteins and ligands, respectively. At tLEaP, the system was also neutralized by adding sodium and chlorine ions. The preparation produced a topology file and the final coordinates of the protein.

Furthermore, minimization was carried out to minimize energy in the system, avoid inappropriate van der Waals contacts (bad contact), and minimize high-energy steric effects to obtain molecules with minimum energy. Energy minimization was carried out using the steepest descent and conjugate gradient algorithms. Minimization was carried out in five steps. The first step was a dynamic constraint of 10 kcal/mol on all atoms. A dynamic constraint of 10 kcal/mol was applied to all atoms except hydrogen in the second step. In the third step, 10 kcal/mol dynamic constraints were applied to the backbone atoms of carbon, alpha carbon (CA), oxygen, and nitrogen. In the fourth step, a dynamic constraint of 10 kcal/mol was applied to the CA atom. Finally, the last step was carried out without any constraints, and the molecules moved freely.

The next stage in this simulation is heating, following the Langevin protocol. This stage uses the NVT dynamic ensemble. The heating was carried out with six temperature ranges, 0–50, 50–100, 100–150, 150–200, 200–250, and 250–300 K. The next stage was an

Table 1. Grid box parameters used for the molecular docking process

Protein target	Grid size A			Spacing (A)	Coordinate		
	x	y	z		x	y	z
COX-2	20	20	20	1.00	-19.163	74.728	33.837

equilibration to stabilize the protein from thermodynamic disturbances in the simulation. The resulting equilibration output was then depicted in a density graph against time using the mdout_analyzer.py command in the Amber20 program. The last stage of the simulation was the production run using the NPT ensemble. The simulation stage of molecule production was made in a natural state without restraints. The production run was carried out for 250 ns.

MD simulations were performed for 250 ns for each COX-2-ligand complex. The atomic coordinates in the complex system were stored at 0.2-ns time intervals during the simulation. Using the initial structure of the MD simulation as the reference structure, the CPPTRAJ module from AmberTools20 was used to determine the RMSD value to validate the convergence of the MD simulation process for calculating hydrogen bonds formed in the ligand-complex during the simulation. In addition, the structural flexibility of the protein was estimated by calculating the fluctuating root-mean-square (RMSF) values. Also, the simulation results were analyzed using binding affinity using molecular mechanics energies with the Poisson-Boltzmann surface area method (MM/PBSA) [20].

Measurement of the inhibitory activity of A. lavenia *and* M. calabura *extracts on COX-2 activity*

The inhibition activity measured toward COX-2 was 50, 70, and 96% ethanol extracts of *A. Lavenia* and *M. calabura*. Various extracting compositions were carried out to obtain semipolar and polar compounds from the samples. *In vitro* studies could be followed by *in silico* studies related to the compounds to be tested computationally. All extracts were measured for their inhibitory activity toward COX-2 *in vitro* using COX-2 (Human) Inhibitor Screening Assay KIT (Cayman Chemical Item No. 701080). The kit directly read PGF2α by measuring PGH2 reduction by $SnCl_2$. PGH2 was produced from a reaction catalyzed by COX-2. Prostanoid products were confirmed by enzyme immunoassay (ELISA) using a broad specific antiserum that binds all major prostaglandin compounds.

The test method following the kit protocol includes a COX-2 reaction procedure consisting of the preparation of a COX-2 reagent and a COX-2 reaction process. The reaction process began with inactivating the COX-2 enzyme by heating it in boiling water for 3 min. Then 950 µL of the reaction buffer was pipetted and put into the initial tube activity and all test tubes. During the process, 10 µL of heme and 10 µL inactive COX-2 were added to tube background, added 10 µL of active COX-2 to tube initial activity and all test tubes, added 10 µL of arachidonic acid to all test tubes, then vortexed and incubated for 2 min before adding 50 µL of 1 M HCl. The test tube contains sample extracts with various concentrations. Into each test tube, 100 mL of $SnCl_2$ solution was added and incubated back for 5 min at room temperature before centrifuging at 4000 rpm to obtain a clear supernatant. The resulting supernatant was diluted before being measured by the ELISA procedure. The ELISA procedure includes preparation of buffer solution, special test reagents, dilution of COX-2 reagent, application to 96 well-plates, and measurements using ELISA spectrophotometer at 405–420 nm wavelengths. A more detailed procedure was in the guidebook COX-2 (Human) Inhibitor Screening Assay kit (Cayman Chemical Item No. 701080).

■ RESULTS AND DISCUSSION

Receptors and Ligands Used

Determination of receptors is the first step in the docking process, which is the COX-2 enzyme in this study. This enzyme plays a pivotal role in synthesizing prostanoids involving prostaglandins and thromboxane from arachidonic acid substrates [21]. The 3D structure of COX-2 was obtained from the Protein Data bank website with the PDB code 5IKR. The structure has two chains, namely the A and B chains with 551 amino acid sequences, and still forms a complex with the mefenamic acid ligand so that it needs to be separated to obtain a pure structure of COX-2 protein [22]. Separating COX-2 protein with ligands has been successfully carried out using VMD software. At this stage, water molecules, solvents, and small non-protein molecules were removed to produce a pure protein structure of COX-2 in the *.pdb format. The COX-2 structural model is shown in Fig. 1. The amino acid residues produced from

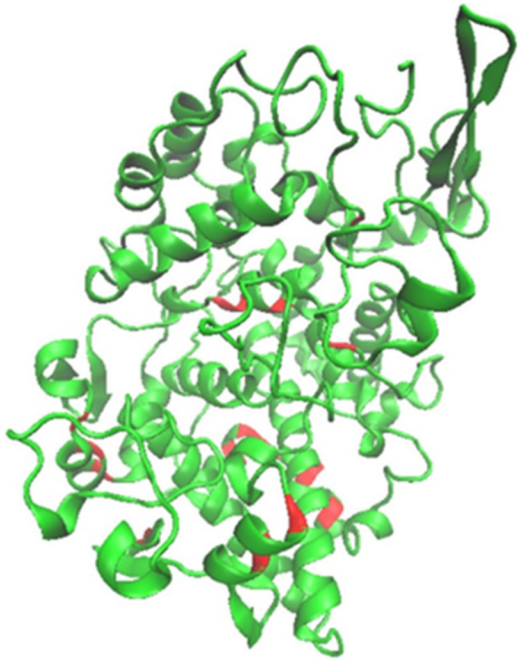

Fig 1. The 3D structure of chain A COX-2 (the red color is the active site of the protein)

the COX-2 structure showed no missing amino acid residues so the COX-2 protein could be used for the docking process. The compounds in *A. Lavenia* and *M. calabura* were referred to in literature [23-24]. Flavonoids, steroids, terpenoids, and saponins are observed in both plants [25].

Molecular Docking Result

Molecular docking is one of the most widely used virtual screening methods by utilizing the 3D structure of a protein, carbohydrates, and nucleic acids. This method can predict the binding affinity between the ligand and protein and the protein-ligand complex structure [7]. The docking process begins with determining the grid box parameters to be used. A grid box is a space or area that will be a place for interaction between ligands and target receptors. Determination of the grid box aims to determine a receptor's active site [26]. Based on the results of docking *A. lavenia* compounds with COX-2, it seems that some compounds have a lower Gibbs free energy value than arachidonic acid, with a binding energy of -7.4 kcal/mol. Arachidonic acid is the main component of lipids in cell membranes. The COX-2 enzyme can metabolize arachidonic acid into various metabolites that trigger an inflammatory response, such as prostaglandins [4].

The results of the COX-2 docking analysis on *A. lavenia* gave the five best compounds with the lowest binding energies (Table 2). The ligands 124 and 149 have the lowest Gibbs free energy among the other test ligands, with a value of -8.7 kcal/mol. It indicates that there has been a strong interaction between COX-2 and these two ligands. The lower the Gibbs free energy value, the more robust and the more stable the interaction between the ligand and the receptor [27]. The energy values of the two ligands were lower than diclofenac. Diclofenac is a positive control used in this study with an -8.1 kcal/mol energy value. Thus, it is shown that the compounds in *A. lavenia* are potential COX-2 inhibitors. Diclofenac is a non-steroidal anti-inflammatory drug from the phenylacetic acid class with anti-inflammatory, analgesic, and antipyretic properties. Diclofenac has high enough selectivity to inhibit COX-2 with greater potency than COX-1 [28].

The results of COX-2 docking with ligands from *M. calabura* are shown in Table 3. The Gibbs free energy of the *M. calabura* ligand has a lower value than the positive control and ligands from *A. lavenia*, meaning higher potential as a COX-2 inhibitor. Ligand 18 has the lowest Gibbs free energy with -9.1 kcal/mol. These results agreed with previous reports that ligand 18 could

Table 2. Gibbs free energy of compound *A. lavenia* with COX-2

Number	Code	Compound	Energy (kcal/mol)
1	124	1a,9b-Dihydro-1H-cyclopropa[a]anthracene	-8.7
2	149	Biphenyl, 3,4-diethyl	-8.7
3	114	3,6-Dimethylphenanthrene	-8.3
4	150	Diclofenac	-8.1
5	110	Z-cyclodecene	-7.2
6	103	Linoleic acid	-7.0

Table 3. Gibbs free energy of compound *M. calabura* with COX-2

Number	Code	Compound	Energy (kcal/mol)
1	18	7-Hydroxyflavone	-9.1
2	30	7-Hydroxyisoflavone	-9.0
3	87	8-Hydroxy-6-methoxyflavone	-9.0
4	14	(2S)-7-Hydroxyflavanone	-8.9
5	19	5,7-Dihydroxyflavone	-8.9
6	150	Diclofenac	-8.1

reduce the production of prostaglandins and other pro-inflammatory mediators in cells induced by lipopolysaccharide [29]. The binding energy values obtained are almost similar to previous studies, which reported that the result of docking COX-2 with eutypoid A compound using Autodock Vina has a binding energy of -9.0 kcal/mol [30]. It indicates that the ligand binds strongly and is very stable to the COX-2 receptor.

Five ligands from Table 3 with the lowest binding energies are compounds that belong to flavonoids. These results agree with previous *in silico* studies related to the docking of flavonoid molecules to COX-2. Quercetin and its derivatives are predicted to have inhibitory activity against COX-2 so that it can be used as an anti-inflammatory [31]. Most flavonoids are known to have anti-inflammatory activity. For example, flavonoids from *Lotus plumule* have been reported to inhibit the production of inflammatory mediators such as NO radicals, PGE2, and TNF-α, as well as pro-inflammatory cytokines IL-1β and IL-6 [1]. The *S. alopecuroides* extract enriched with flavonoids can inhibit the release of lipopolysaccharide-induced NO, PGE2, TNF-α, interleukin-6, and interleukin-1β, and can reduce the expression of iNOS and COX-2 proteins [32]. A mixture of flavonoids and isolated compounds from *Boldoa purpurascens* leaves has been shown to have an anti-inflammatory impact because it can reduce the expression of COX-2 when induced with lipopolysaccharides [33].

Characteristic of ligands according to Lipinski's rule

Lipinski's rule concerns the absorption or permeation of a drug molecule. A drug molecule that has a deviation from the Lipinski rule can have poor absorption in the body. Lipinski's rules include that the molecular weight should not exceed 500 g/mol, have a log *P* value not greater than five, have a hydrogen bond donor of less than five, and a hydrogen acceptor of less than 10 [34]. Based on Table 4, three compounds of *A. lavenia*, namely ligands 114, 124, and 149, have Lipinski rule deviations related to the log *P* value of more than five. The log *P* value indicates the lipophilicity of a molecule [35]. Lipophilicity affects solubility and affects permeability, potency, selectivity, distribution, metabolism, excretion, and toxicity. Its high lipophilicity ($\log P > 5$) often contributes to its low solubility and poor drug absorption. In addition, highly lipophilic compounds tend to bind to hydrophobic molecules in the body other than their intended targets, increasing the risk of toxicity to cells or tissues [36]. According to Lipinski's rule, ligands 18, 30, and 87 have good properties

Table 4. Ligand characteristic of *A. lavenia* and *M. calabura* based on Lipinski's rule

Compound	Molecular weight (g/mol)	Log *P*	Number of hydrogen bond donors	Number of hydrogen bond acceptors
18	238.24	1.66	1	3
30	238.24	1.66	1	3
87	268.26	1.33	1	4
114	206.28	5.67	0	0
124	192.26	5.15	0	0
149	210.31	5.83	0	0

as drug molecules. The three ligands do not have Lipinski rule deviations to have good absorption or permeation in the body as drug molecules.

Prediction of ligand toxicity

A new drug molecule is expected to have better activity and lower toxicity than the existing drugs. Therefore, the ligands with the three lowest binding energies of *A. lavenia* and *M. calabura* were determined first for their toxicity. Then, a ligand toxicity test was carried out using Data Warrior software. Several studies have used this software to find new medicinal compounds, such as cancer and antidepressant drugs [37-38]. The results of the predictive analysis of ligand toxicity using Data Warrior are shown in Table 5 [39]. The ligands 18, 30, and 87 of *M. calabura*, and ligand 124 of *A. lavenia*, have no mutagenic, tumorigenic, irritant, and reproductive effects. Therefore, it indicates that the two plants have potential as COX-2 inhibitor agents. However, ligands 114 and 149 have a low tumorigenic effect, so they can cause cancer if taken for a long time as a drug.

Ligand-receptor interaction analysis

The ligand-receptor interaction was carried out on the ligands with the lowest binding energies of the two plants. Ligand interaction analysis was performed using DS Visualizer. This analysis was carried out to see the active site and the type of bond between the ligand and the amino acid residues contained in COX-2. Interactions are hydrogen bonds, electrostatic interactions, and van der Waals interactions. The interaction between ligand 18 and COX-2 amino acid residues is shown in Fig. 2. The interaction of ligand 18

Table 5. Ligand properties of *A. lavenia* and *M. calabura* based on toxicity

Compound	Effect			
	Mutagenic	Irritant	Tumorigenic	Reproductive
18	None	None	None	None
30	None	None	None	None
87	None	None	None	None
114	Low	None	Low	None
124	None	None	None	None
149	None	None	Low	None

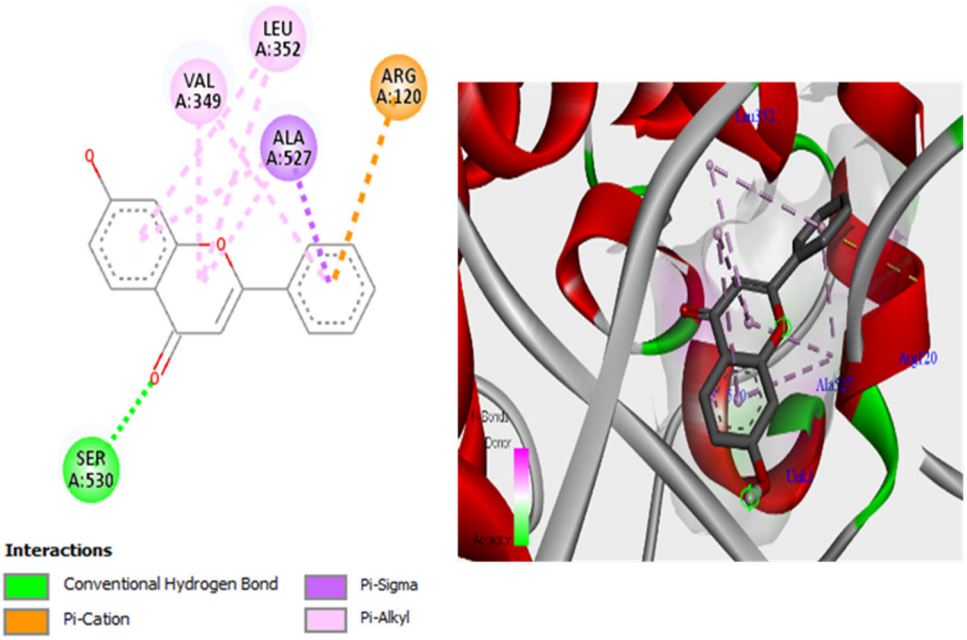

Fig 2. Ligand 18 interaction with COX-2 in 2D (left) and 3D (right)

produces hydrogen bonds at the Ser530 residue, in addition to hydrogen bonding, hydrophobic interactions at residues Arg120, Val349, Leu352, and Ala527. The results so far are still in line with previous studies related to the active site of COX-2. The results of previous studies reported that COX-2 protein has an active site on the amino acid residues Ser530, Ala527, Gly526, Met522, and Leu352 [40]. The binding between the ligand and the active site of COX-2 can change the secondary or tertiary structure of the COX-2 protein. Changes in the protein structure make COX-2 unable to recognize its substrate to produce prostaglandin inflammatory mediators [41]. An article reported that arachidonic acid interacts with COX-2 at the amino acid residues Tyr385, Ser530, Arg120, Leu531, Val349, Ser353, Ile523, Ala527, Leu352, Gly526, Phe205, Phe209, Val-228, Val-344, Ile-377, Phe-381, Gly533, and Leu-534 [42]. Tyr-385 is a critical catalytic residue that donates a hydrogen atom to heme during enzyme activation. In addition, the amino acid residue Ser530 has a vital role in the inhibition of COX-2 activity [43].

The analysis of ligand 124 with COX-2 (Fig. 3) shows hydrophobic interactions at the amino acid residues Val349, Leu352, Trp387, Phe518, Met522, Val523, Gly526, and Ala527. Hydrophobic interactions are between the ligand molecule's non-polar group and the receptor's non-polar region. Hydrophobic interactions can stabilize the ligand-receptor interaction by lowering the value of the Gibbs free energy because the interaction is a combination of weakly interacting bonds such as van der Waals, dipole-dipole, and electrostatic bonds [44]. Therefore, the Gibbs free energy value of ligand 18 is lower due to the hydrogen interaction at the amino acid residue Ser530 than ligand 124, which does not have hydrogen interactions.

Molecular Dynamics Result

A total of 10 ligands consisting of five ligands each from *A. lavenia* and *M. calabura* (Table 6) were selected based on the lowest binding energy resulting from the molecular docking process for stability through MD

Table 6. List of ligands selected for MD simulation of stability

Number	Code	Compound
1	14	(2S)-7-Hydroxyflavanone
2	18	7-Hydroxyflavone
3	19	5,7-Dihydroxyflavone
4	30	7-Hydroxyisoflavone
5	87	8-Hydroxy-6-methoxyflavone
6	103	Linoleic acid
7	110	Z-cyclodecene
8	114	3,6-Dimethylphenanthrene
9	124	1a,9b-Dihydro-1H-cyclopropa[a]anthracene
10	149	Biphenyl, 3,4-diethyl

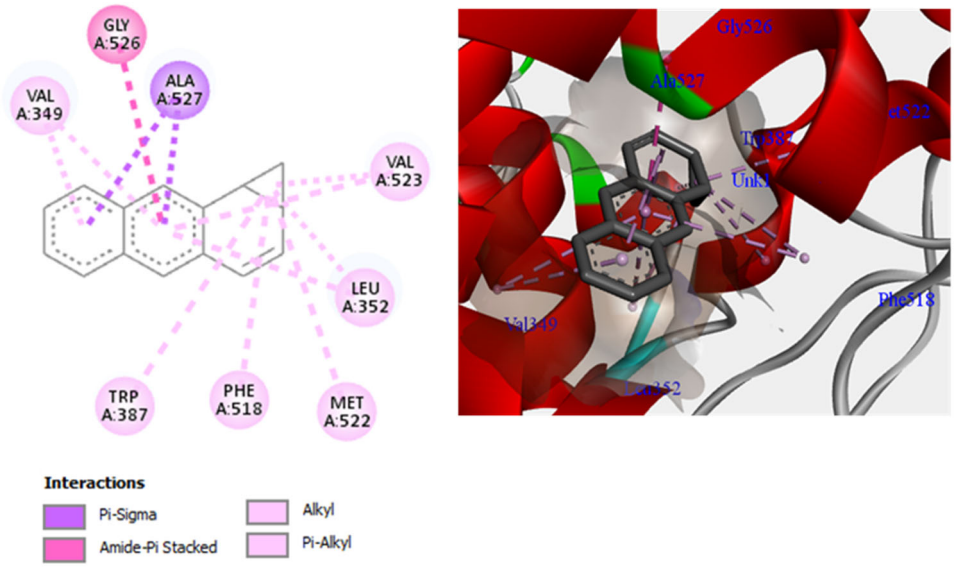

Fig 3. Ligand 124 interaction with COX-2 in 2D (left) and 3D (right)

simulation for 250 ns. The RMSD values for compounds from *A. lavenia* increased during the first 50 ns. After that phase, the five ligands experienced simple fluctuations in the range of 1.5–2.5 Å and had an average RMSD below 2 Å (Fig. 4). Overall, in the 250 ns period, the COX-2 complex structure with five selected *A. lavenia* ligands converged because the fluctuations in the RMSD value produced were not too large (not exceeding 1.5 Å). It indicates that the complex formed is stable during the simulation [45]. Based on Fig. 5, the COX-2 complex with the *M. calabura* ligand looks stable at the beginning of the simulation until it reaches a simulation time of 125 ns, the RMSD value increases until the end of the simulation, especially in the 8-hydroxy-6-methoxyflavone ligand. The COX-2 complex with 8-hydroxy-6-methoxyflavone ligand has the most considerable fluctuation in the RMSD value among the other four ligand complexes with a range of 0.96–3.14 Å. Fig. 5 exhibits a decrease in the stability of the COX-2 complex with 8-hydroxy-6-methoxyflavone at the end of the simulation. However, overall, the five ligand complexes of *M. calabura* have good stability during the simulation because the fluctuations produced are not too large (still close to 1.5 Å).

The RMSF value indicates the flexibility of the receptor amino acid residues. Changes in the RMSF value can explain fluctuations in each residue in the protein structure and protein flexibility during the MD simulation. RMSF of the two species ligands has almost the same value seen from the peaks and valleys formed (Fig. 6). RMSF value fluctuates at amino acid residues

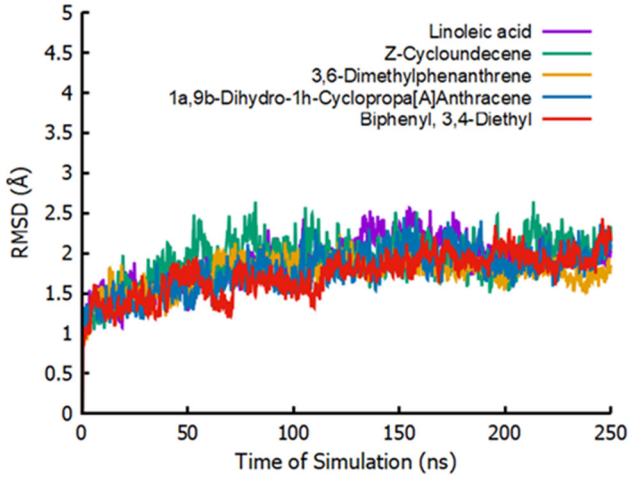

Fig 4. RMSD of the protein-ligand complex from *A. lavenia* at 250 ns

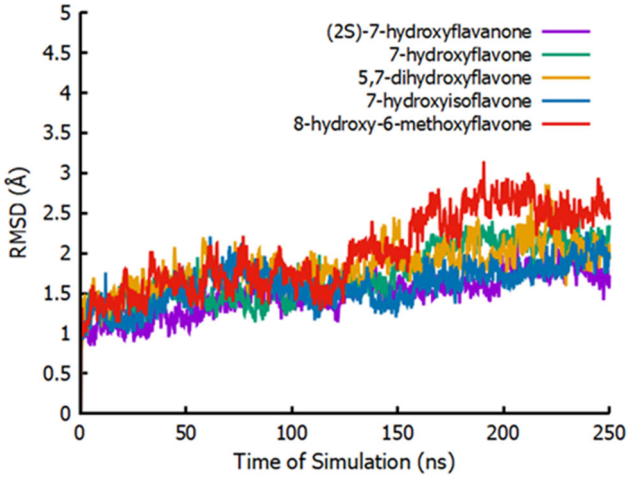

Fig 5. RMSD of the protein-ligand complex from *M. calabura* at 250 ns

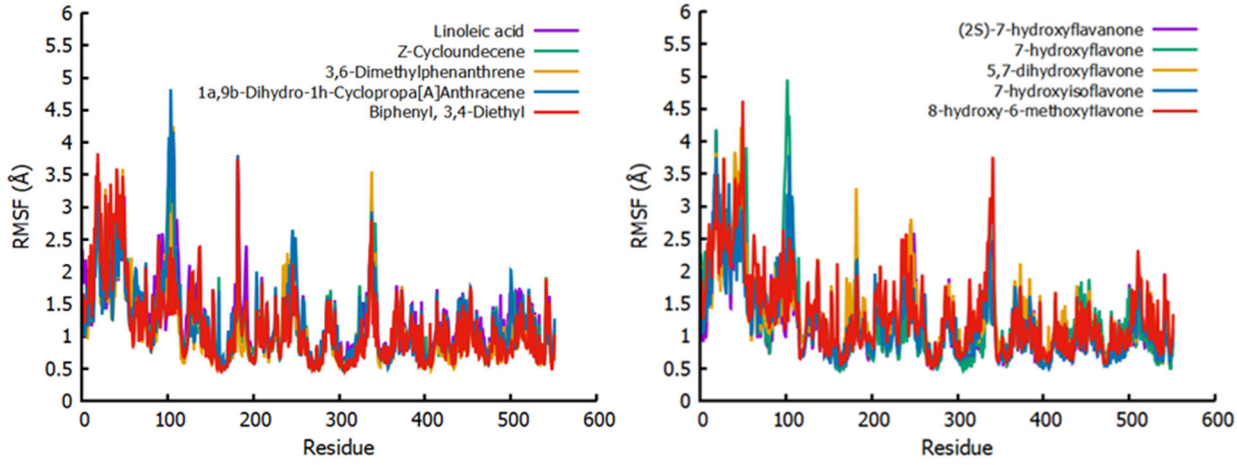

Fig 6. RMSF of the protein-ligand complex from *A. lavenia* (left) and *M. calabura* (right) at 250 ns

15–30, 40–54, 100–110, and 335–342. Higher RMSF values indicate greater flexibility during MD simulations [46]. Amino acid residues 100–110 give the highest RMSF fluctuations peaks because they do not bond with the ligands, causing the amino acid residues to become more flexible.

In comparison, the valleys indicate that the ligand interacts with the residue causing the COX-2 protein to become more rigid [47]. Residues above 350 are also related to the active site of COX-2, which is in the amino acid residues Ser530, Ala527, Gly526, Met522, and Leu352 [39]. In all complexes, the RMSF value for each residue surrounding the ligand has a lower value of less than 1 Å, as shown in residues above 350. The interaction between the ligand and protein is relatively stable during the MD simulation.

The calculation of the binding energy of the protein-ligand complex was carried out using the MMPBSA technique. This calculation technique can provide information about the stability of the bond between the ligand and COX-2 as a complex structure. Based on Fig. 7, the linoleic acid compound had the lowest MMPBSA value with an average energy of -48.605 kcal/mol. The Z-cycloundecene ligand had the highest binding energy with an average energy of -28.733 kcal/mol. It shows a very different order of results from the Gibbs free energy in the molecular docking step, as clearly seen in Table 7 and 8. The difference in the data can represent that molecular docking data needs to be validated using molecular dynamics simulations because logarithms and conditions applied in molecular docking simulations with Autodock Vina are more straightforward and more rigid.

In contrast, the receptors are flexible in molecular dynamics simulations. Hence, more parameters are required, and the logarithm of applied calculations is more complex than in molecular docking. The parameters used in the computation of MMPBSA that do not exist in the molecular docking include the dielectric constant, parameters for non-polar energy, polar solvation energy, radius, electrostatic energy, and entropy of the system used. As a result, the calculation of the MMPBSA value has better accuracy than the calculation by molecular docking [48]. Meanwhile, the results of MMPBSA with *M. calabura* ligand (Fig. 8) have energy that is almost similar to energy fluctuations ranging from -30 to -40 kcal/mol. Ligand 8-hydroxy-6-methoxyflavone has the most negative average binding energy of -38.346 kcal/mol. The negative Gibbs free energy value indicates that the receptor has an attractive interaction with the ligand. Furthermore, the value of the Gibbs free energy of the ligand pair in each conformation is negative, signifying that the receptor with the ligand has a stable bond [49].

Hydrogen bond analysis was also performed on the MD Trajectory to calculate the number of hydrogen bonds formed in each complex during the simulation.

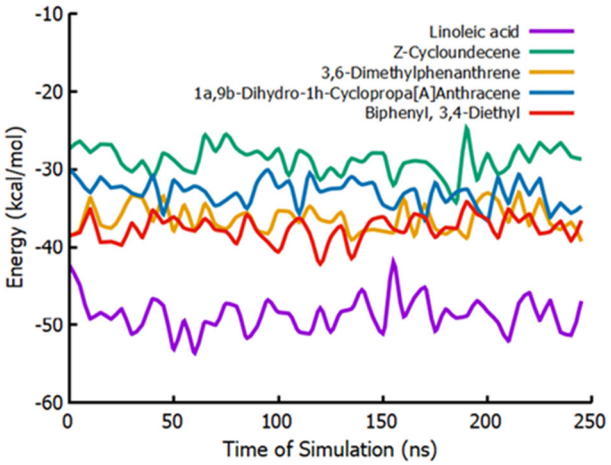

Fig 7. MM-PBSA of the protein-ligand complex from *A. lavenia* at 250 ns

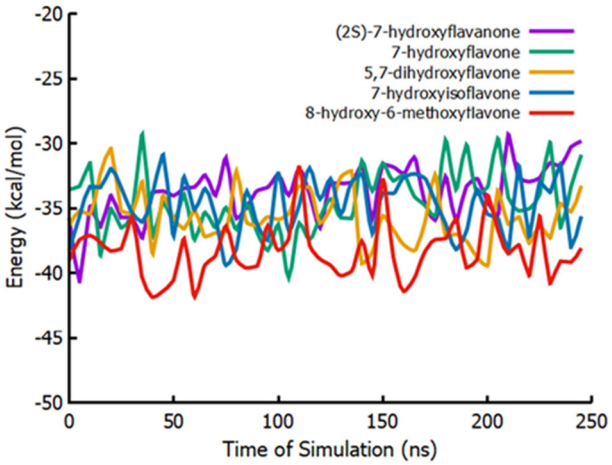

Fig 8. MM-PBSA of the protein-ligand complex from *M. calabura* at 250 ns

Table 7. Comparison of energy from Autodock Vina and MMPBSA from *A. lavenia*

Code	Compound	Energy (kcal/mol)	
		Autodock Vina	MMPBSA
124	1a,9b-Dihydro-1H-cyclopropa[a]anthracene	-8.7	-33.0
149	Biphenyl, 3,4-diethyl	-8.7	-37.6
114	3,6-Dimethylphenanthrene	-8.3	-36.3
110	Z-cyclodecene	-7.2	-28.7
103	Linoleic acid	-7.0	-48.6

Table 8. Comparison of energy from Autodock Vina and MMPBSA from *M. calabura*

Code	Compound	Energy (kcal/mol)	
		Autodock Vina	MMPBSA
18	7-Hydroxyflavone	-9.1	-34.5
30	7-Hydroxyisoflavone	-9.0	-34.7
87	8-Hydroxy-6-methoxyflavone	-9.0	-38.3
14	(2S)-7-Hydroxyflavanone	-8.9	-33.6
19	5,7-Dihydroxyflavone	-8.9	-35.7

From *A. lavenia*, only linoleic acid ligands form hydrogen bonds with two hydrogen bonds on average (Fig. 9). The other four ligands do not show hydrogen bonding. The hydrogen bond is not formed presumably because the position of the donor atom and the hydrogen acceptor are far apart at the time of docking, avoiding hydrogen bonds between COX-2 and the ligand. It makes linoleic acid ligands have the lowest binding energy than the other four due to hydrogen bonds with COX-2. Hydrogen bonds can strengthen the interactions between ligands and proteins. H-bonds are critical for protein folding and protein-ligand interactions [50]. These results are consistent with the docking analysis that the ligand 1a,9b-dihydro-1H-cyclopropa[a]anthracene does not form hydrogen interactions with COX-2 but forms hydrophobic interactions to stabilize the complex structure formed.

In contrast to the ligands from *A. lavenia*, varying hydrogen bonds are formed between the ligands on *M. calabura* and COX-2 (Fig. 10). Ligands (2S)-7-hydroxyflavanone and 8-hydroxy-6-methoxyflavone

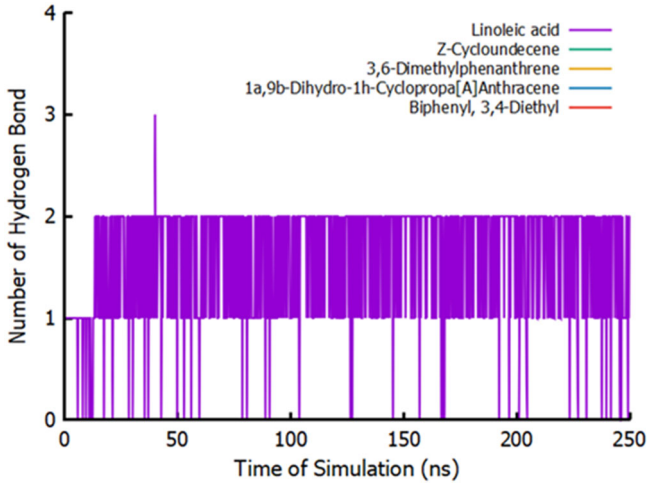

Fig 9. Number of hydrogen bonds formed for the MD simulation trajectory for the COX-2 enzyme with selected ligand from *A. lavenia*

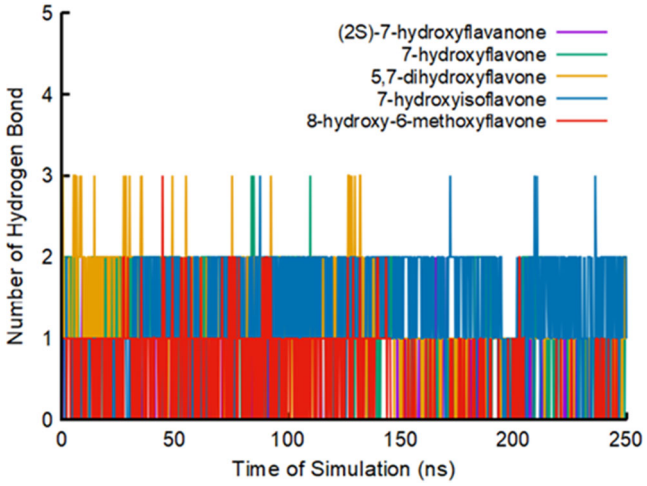

Fig 10. Number of hydrogen bonds formed for the MD simulation trajectory for the COX-2 enzyme with selected ligand from *M. calabura*

formed one hydrogen bond with COX-2 from the beginning of the simulation to the end of the MD simulation. The 7-hydroxyisoflavone ligand most often forms two hydrogen bonds during the simulation, and sometimes three hydrogen bonds can be formed even if only temporarily. Meanwhile, according to the molecular docking analysis, 7-hydroxy flavone only formed one hydrogen bond. The 5,7-dihydroxyflavone ligand formed two hydrogen bonds at the beginning of the simulation and three hydrogen bonds formed during the MD simulation.

In vitro Extract Inhibition Test against COX-2

The samples measured for their inhibitory activity on COX-2 were single extracts of *A. lavenia* and *M. calabura* with 25, 100, and 1000 ppm concentrations. The extract was produced by macerating the samples for 3 × 24 h in 50, 70, and 96% ethanol as the solvent. Referring to Fig. 11, the 50% EtOH extract does not show inhibition of COX-2 activity. The inhibitory activity of 70% EtOH extract is only seen at a concentration of 100 ppm with an inhibition value of 6%, and 1000 ppm is equal to 81%. The 96% EtOH extract gives a high inhibitory power to COX-2 activity. The 96% EtOH extract of *A. lavenia* with 25 and 100 ppm concentrations produced an inhibitory power of about 98%. These results are consistent with the previous *in vivo* studies that *A. lavenia* extract can treat the pathogenesis of pneumonia in LPS-induced rats. In addition, the extract can reduce MAPK and NF-kB activity to suppress the production of pro-inflammatory cytokines [11]. The compound ent-11α-hydroxy-15-oxo-kaur-16-en-19-oic-acid in *A. lavenia* is also reported to inhibit NF-kB expression in the treatment of colorectal cancer [51]. Several groups of compounds that have been known to have potential as COX-2 inhibitors include acetogenins [52], alkaloids [53], and sterol derivatives [54].

The inhibitory power of EtOH single extract of *M. calabura* is shown in Fig. 12. In contrast to *A. lavenia*, 50% EtOH extract with a concentration of 25 ppm could inhibit COX-2. It showed the highest inhibitory power of 50% EtOH extract of 51% at a concentration of 1000 ppm. The inhibitory activity above 50% is given by 70% and 96% EtOH extracts. At 25 ppm concentration, both 70 and 96% EtOH extracts can provide inhibition power approaching 80 and 84%, respectively. EtOH 70 and 96% extracts may inhibit COX-2 activity up to 100% at 1000 ppm concentration. Compared with the other two EtOH extracts, the inhibitory power of 96% EtOH extract shows a higher potential for COX-2 inhibition.

The positive control employed in this study is diclofenac, a synthetic drug commonly used as an anti-inflammatory. Based on the research results, diclofenac has a COX-2 inhibition percentage of 88% at a concentration of 0.75 ppm (Fig. 13). The inhibitory activity produced by all tested extracts was able to compete

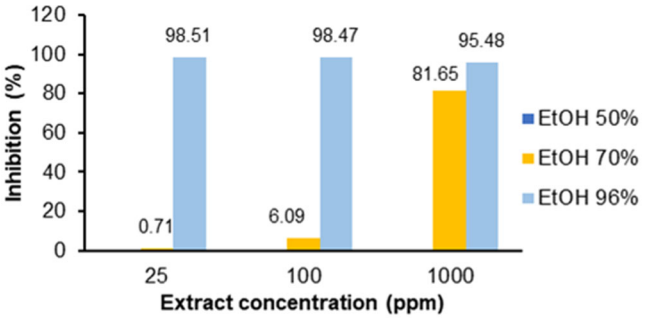

Fig 11. Inhibition of EtOH extract of *A. lavenia* on COX-2 activity

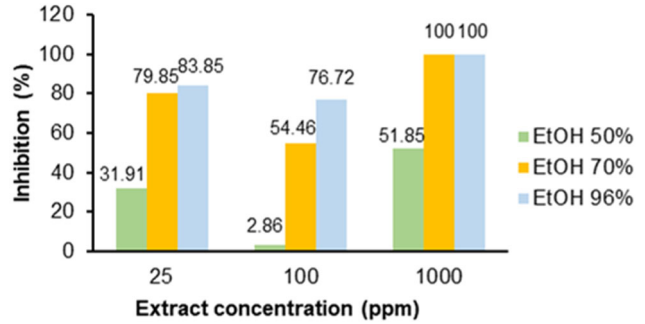

Fig 12. The inhibitory activity of the EtOH extract of *M. calabura* on COX-2

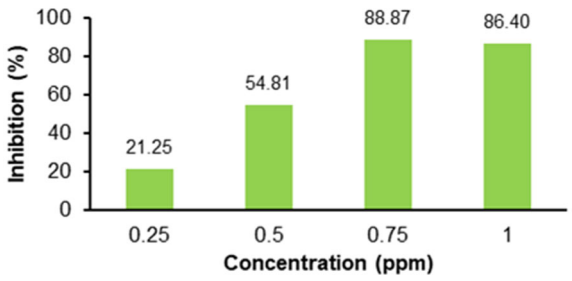

Fig 13. The inhibitory activity of diclofenac on COX-2

with diclofenac as a positive control even though the concentration of the extract used was relatively different. The anti-inflammatory activity becomes better if the required concentration is getting smaller. Based on the measurement of the inhibition of COX-2, both plants have the potential to be anti-inflammatory.

The active compounds found in extracts of *A. lavenia* and *M. calabura*, which act as anti-inflammatory through inhibition of COX-2 activity, are flavonoids and steroids. Following *in silico* results, the five compounds from *M. calabura*, with the lowest Gibbs free energy, belong to flavonoids. Flavonoids can suppress COX gene expression through cell signaling pathways such as the NF-B pathway and tyrosine kinase, but the mechanism has not been determined with certainty [55]. However, based on the *in silico* results, it can be predicted that the compounds contained in the extracts of *A. lavenia* and *M. calabura* will interact with COX-2 in the body. It happens because, in the inflammatory process, COX-2 production will increase so that the potential for binding between the active compounds in the extracts of these two species with COX will be even more significant. This interaction can inhibit COX-2 in binding arachidonic acid so that the catalysis process does not occur and can result in changes in the structure and active site of the enzyme so that COX-2 cannot catalyze the formation of prostaglandins.

■ CONCLUSION

We conclude that *A. lavenia* and *M. calabura* extracts have the potency to inhibit the performance of COX-2, which affects the regulation of inflammation *in vitro*. The computational simulations agree with the *in vitro* experiment results that show an interaction between the compounds in both plants and the active site of the COX-2 enzyme. Furthermore, the MD simulations show that the interactions between COX-2 and ten selected compounds formed a stable protein-ligand complex. These results provide an urgently needed opportunity to develop new therapeutic drug design and discovery strategies to treat inflammation.

■ ACKNOWLEDGMENTS

The authors would like to thank the Ministry of Education and Culture, Research and Technology of the Republic of Indonesia for granting this work through *Penelitian Terapan Kompetitif Nasional* scheme (Grant Number 2052/IT3.L1/PN/2021. The Authors also acknowledge computational resources provided by the HPC Lab of Theoretical Physics Division, Department of Physics, IPB University.

■ AUTHOR CONTRIBUTIONS

Bagaskoro Tuwalaid, Dyah Iswantini, and Setyanto Tri Wahyudi conducted the experiment. Bagaskoro Tuwalaid wrote the manuscript and conducted the scoring docking analysis and simulation of molecular dynamics. Dyah Iswantini and Setyanto Tri Wahyudi supervised the experimental and revised the manuscript. All authors agreed to the final version of this manuscript.

■ REFERENCES

[1] Chen, L., Deng, H., Cui, H., Fang, J., Zuo, Z., Deng, J., Li, Y., Wang, X., and Zhao, L., 2018, Inflammatory responses and inflammation-associated diseases in organs, *Oncotarget*, 9 (6), 7204–7218.

[2] Merad, M., and Martin, J.C., 2020, Author correction: Pathological inflammation in patients with COVID-19: A key role for monocytes and macrophages, *Nat. Rev. Immunol.*, 20 (7), 448.

[3] Syahputra, G., Ambarsari, L., and Sumaryada, T., 2014, Simulasi docking kurkumin enol, bisdemetoksikurkumin dan analognya sebagai inhibitor enzim12-lipoksigenase, *J. Biofisika*, 10 (1), 55–67.

[4] Wang, T., Fu, X., Chen, Q., Patra, J.K., Wang, D., Wang, Z., and Gai, Z., 2019, Arachidonic acid metabolism and kidney inflammation, *Int. J. Mol. Sci.*, 20 (15), 3683.

[5] Wongrakpanich, S., Wongrakpanich, A., Melhado, K., and Rangaswami, J., 2018, A comprehensive review of non-steroidal anti-inflammatory drug use in the elderly, *Aging Dis.*, 9 (1), 143–150.

[6] Saikia, S., and Bordoloi, M., 2019, Molecular docking: Challenges, advances and its use in drug discovery perspective, *Curr. Drug Targets*, 20 (5), 501–521.

[7] Salmaso, V., and Moro, S., 2018, Bridging molecular docking to molecular dynamics in exploring ligand-protein recognition process: An overview, *Front. Pharmacol.*, 9, 923.

[8] Ravindranath, P.A., Forli, S., Goodsell, D.S., Olson, A.J., and Sanner, M.F., 2015, AutoDockFR: Advances in protein-ligand docking with explicitly specified binding site flexibility, *PLOS Comput. Biol.*, 11 (12), e1004586.

[9] De Vivo, M., Masetti, M., Bottegoni, G., and Cavalli, A., 2016, Role of molecular dynamics and related methods in drug discovery, *J. Med. Chem.*, 59 (9), 4035–4061.

[10] Case, D.A., Cheatham, T.E., Darden, T., Gohlke, H., Luo, R., Merz, K.M., Onufriev, A., Simmerling, C., Wang, B., and Woods, R.J., 2005, The Amber biomolecular simulation programs, *J. Comput. Chem.*, 26 (16), 1668–1688.

[11] Chen, J.J., Deng, J.S., Huang, C.C., Li, P.Y., Liang, Y.C., Chou, C.Y., and Huang, G.J., 2019, *p*-Coumaric-acid-containing *Adenostemma lavenia* ameliorates acute lung injury by activating AMPK/Nrf2/HO-1 signaling and improving the anti-oxidant response, *Am. J. Chin. Med.*, 47 (7), 1483–1506.

[12] Cheng, P.C., Hufford, C.D., and Doorenbos, N.J., 1979, Isolation of 11-hydroxyated kauranic acids from *Adenostemma lavenia*, *J. Nat. Prod.*, 42 (2), 183–186.

[13] Lin, J.T., Chang, Y.Y., Chen, Y.C., Shen, B.Y., and Yang, D.J., 2017, Molecular mechanisms of the effects of the ethanolic extract of *Muntingia calabura* Linn. fruit on lipopolysaccharide-induced pro-inflammatory mediators in macrophages, *Food Funct.*, 8 (3), 1245–1253.

[14] Pettersen, E.F., Goddard, T.D., Huang, C.C., Couch, G.S., Greenblatt, D.M., Meng, E.C., and Ferrin, T.E., 2004, UCSF Chimera—A visualization system for exploratory research and analysis, *J. Comput. Chem.*, 25 (13), 1605–1612.

[15] Morris, G.M., Huey, R., and Olson, A.J., 2008, Using AutoDock for Ligand-Receptor Docking, *Curr. Protoc. Bioinf.*, 24 (1), 8.14.1–8.14.40.

[16] Zubair, M.S., Anam, S., Maulana, S., and Arba, M., 2021, *In vitro* and *in silico* studies of quercetin and daidzin as selective anticancer agents, *Indones. J. Chem.*, 21 (2), 310–317.

[17] Gordon, J.C., Myers, J.B., Folta, T., Shoja, V., Heath, L.S., and Onufriev, A., 2005, H++: A server for estimating pK_as and adding missing hydrogens to macromolecules, *Nucleic Acids Res.*, 33 (Suppl. 2), W368–W371.

[18] Myers, J., Grothaus, G., Narayanan, S., and Onufriev, A., 2006, A simple clustering algorithm can be accurate enough for use in calculations of pKs in macromolecules, *Proteins: Struct., Funct., Bioinf.*, 63 (4), 928–938.

[19] Anandakrishnan, R., Aguilar, B., and Onufriev, A.V., 2012, H++ 3.0: Automating pK prediction and the preparation of biomolecular structures for atomistic molecular modeling and simulations, *Nucleic Acids Res.*, 40 (W1), W537–W541.

[20] Radwan, A., and Mahrous, G.M., 2020, Docking studies and molecular dynamics simulations of the binding characteristics of waldiomycin and its methyl ester analog to *Staphylococcus aureus* histidine kinase, *PLoS One*, 15 (6), e0234215.

[21] Rawat, C., Kukal, S., Dahiya, U.R., and Kukreti, R., 2019, Cyclooxygenase-2 (COX-2) inhibitors: Future therapeutic strategies for epilepsy management, *J. Neuroinflammation*, 16 (1), 197.

[22] Orlando, B.J., and Malkowski, M.G., 2016, Substrate-selective inhibition of cyclooxygeanse-2 by fenamic acid derivatives is dependent on peroxide tone, *J. Biol. Chem.*, 291 (29), 15069–15081.

[23] Fauzan, A., Praseptiangga, D., Hartanto, R., and Pujiasmanto, B., 2018, Characterization of the chemical composition of *Adenostemma lavenia* (L.) Kuntze and *Adenostemma platyphyllum* Cass, *IOP Conf. Ser.: Earth Environ. Sci.*, 102, 012029.

[24] Mahmood, N.D., Nasir, N.L.M., Rofiee, M.S., Tohid, S.F.M., Ching, S.M., Teh, L.K., Salleh, M.Z., and Zakaria, Z.A., 2014, *Muntingia calabura*: A review of its traditional uses, chemical properties, and pharmacological observations, *Pharm. Biol.*, 52 (12), 1598–1623.

[25] Krishnaveni, M., and Dhanalakshmi, R., 2014, Qualitative and quantitative study of

phytochemicals in *Muntingia calabura* L. leaf and fruit, *World J. Pharm. Res.*, 3 (6), 1687–1696.

[26] Rachmania, R.A., Supandi, S., and Cristina, F.A.D., 2016, Analisis penambatan molekul senyawa flavonoid buah mahkota dewa (*Phaleria macrocarpa* (Scheff.) Boerl.) pada reseptor α-glukosidase sebagai antidiabetes, *Pharm. J. Indones.*, 13 (2), 239–251.

[27] Legiawati, L., Fadilah, F., Bramono, K., and Indriatmi, W., 2018, *In silico* study of Centella asiatica active compounds as anti-inflammatory agent by decreasing IL-1 and IL-6 activity, promoting IL-4 activity, *J. Pharm. Sci. Res.*, 10 (9), 2142–2147.

[28] Altman, R., Bosch, B., Brune, K., Patrignani, P., and Young, C., 2015, Advances in NSAID development: Evolution of diclofenac products using pharmaceutical technology, *Drugs*, 75 (8), 859–877.

[29] Jin, Z., Yang, Y.Z., Chen, J.X., and Tang, Y.Z., 2017, Inhibition of pro-inflammatory mediators in RAW264.7 cells by 7-hydroxyflavone and 7,8-dihydroxyflavone, *J. Pharm. Pharmacol.*, 69 (7), 865–874.

[30] Taidi, L., Maurady, A., and Britel, M.R., 2022, Molecular docking study and molecular dynamic simulation of human cyclooxygenase-2 (COX-2) with selected eutypoids, *J. Biomol. Struct. Dyn.*, 40 (3), 1189–1204.

[31] Kartasasmita, R.E., Herowati, R., Harmastuti, N., and Gusdinar, T., 2009, Quercetin derivatives docking based on study of flavonoids interaction to cyclooxygenase-2, *Indones. J. Chem.*, 9 (2), 297–302.

[32] Guo, C., Yang, L., Wan, C.X., Xia, Y.Z., Zhang, C., Chen, M.H., Wang, Z.D., Li, Z.R., Li, X.M., Geng, Y.D., and Kong, L.Y., 2016, Anti-neuroinflammatory effect of Sophoraflavanone G from *Sophora alopecuroides* in LPS-activated BV2 microglia by MAPK, JAK/STAT and Nrf2/HO-1 signaling pathways, *Phytomedicine*, 23 (13), 1629–1637.

[33] González Mosquera, D.M., Hernández Ortega, Y., Fernández, P.L., González, Y., Doens, D., Vander Heyden, Y., Foubert, K., and Pieters, L., 2018, Flavonoids from *Boldoa purpurascens* inhibit proinflammatory cytokines (TNF-α and IL-6) and the expression of COX-2, *Phytother. Res.*, 32 (9), 1750–1754.

[34] Lipinski, C.A., Lombardo, F., Dominy, B.W., and Feeney, P.J., 2001, Experimental and computational approaches to estimate solubility and permeability in drug discovery and development settings, *Adv. Drug Delivery Rev.*, 46 (1-3), 3–26.

[35] Gao, Y., Gesenberg, C., and Zheng, W., 2017, "Oral Formulations for Preclinical Studies: Principle, Design, and Development Considerations" in *Developing Solid Oral Dosage Forms*, 2nd Ed., Eds. Qiu, Y., Chen, Y., Zhang, G.G.Z., Yu, L., and Mantri, R.V., Academic Press, Boston, US, 455–495.

[36] Hughes, J.D., Blagg, J., Price, D.A., Bailey, S., DeCrescenzo, G.A., Devraj, R.V., Ellsworth, E., Fobian, Y.M., Gibbs, M.E., Gilles, R.W., Greene, N., Huang, E., Krieger-Burke, T., Loesel, J., Wager, T., Whiteley, L., and Zhang, Y., 2008, Physiochemical drug properties associated with *in vivo* toxicological outcomes, *Bioorg. Med. Chem. Lett.*, 18 (17), 4872–4875.

[37] Ajay Kumar, T.V., Kabilan, S., and Parthasarathy, V., 2017, Screening and toxicity risk assessment of selected compounds to target cancer using QSAR and pharmacophore modelling, *Int. J. PharmTech Res.*, 10 (4), 219–224.

[38] Sultan, M.A., Galil, M.S.A., Al-Qubati, M., Omar, M.M., and Barakat, A., 2020, Synthesis, molecular docking, druglikeness analysis, and ADMET prediction of the chlorinated ethanoanthracene derivatives as possible antidepressant agents, *Appl. Sci.*, 10 (21), 7727.

[39] Sander, T., Freyss, J., von Korff, M., and Rufener, C., 2015, DataWarrior: An open-source program for chemistry aware data visualization and analysis, *J. Chem. Inf. Model.*, 55 (2), 460–473.

[40] Reddy, K.K., Vidya Rajan, V.K., Gupta, A., Aparoy, P., and Reddanna, P., 2015, Exploration of binding site pattern in arachidonic acid metabolizing enzymes, cyclooxygenases and lipoxygenases, *BMC Res. Notes*, 8 (1), 152.

[41] Wang, B., Wu, L., Chen, J., Dong, L., Chen, C., Wen,

Z., Hu, J., Fleming, I., and Wang, D.W., 2021, Metabolism pathways of arachidonic acids: Mechanisms and potential therapeutic targets, *Signal Transduction Targeted Ther.*, 6 (1), 94.

[42] Rouzer, C.A., and Marnett, L.J., 2020, Structural and chemical biology of the interaction of cyclooxygenase with substrates and non-steroidal anti-inflammatory drugs, *Chem. Rev.*, 120 (15), 7592–7641.

[43] Deb, P.K., Mailabaram, R.P., Al-Jaidi, B., and Saadh, M.J., 2017, "Molecular Basis of Binding Interactions of NSAIDs and Computer-Aided Drug Design Approaches in the Pursuit of the Development of Cyclooxygenase-2 (COX-2) Selective Inhibitors" in *Nonsteroidal Anti-Inflammatory Drugs*, Eds. Al-kaf, A.G., IntechOpen, Rijeka, Croatia.

[44] Syahputra, G., 2014, Simulasi Docking Senyawa Kurkumin dan Analognya sebagai Inhibitor Enzim 12-Lipoksigenase, *Thesis*, Institut Pertanian Bogor.

[45] Mahapatra, M.K., Bera, K., Singh, D.V., Kumar, R., and Kumar, M., 2018, *In silico* modelling and molecular dynamics simulation studies of thiazolidine based PTP1B inhibitors, *J. Biomol. Struct. Dyn.*, 36 (5), 1195–1211.

[46] Zhao, Y., Zeng, C., and Massiah, M.A., 2015, Molecular dynamics simulation reveals insights into the mechanism of unfolding by the A130T/V mutations within the MID1 zinc-binding Bbox1 domain, *PLoS One*, 10 (4), e0124377.

[47] Khan, S., Farooq, U., and Kurnikova, M., 2017, Protein stability and dynamics influenced by ligands in extremophilic complexes – A molecular dynamics investigation, *Mol. Biosyst.*, 13 (9), 1874–1887.

[48] Genheden, S., and Ryde, U., 2015, The MM/PBSA and MM/GBSA methods to estimate ligand-binding affinities, *Expert Opin. Drug Discovery*, 10 (5), 449–461.

[49] Botelho, F.D., dos Santos, M.C., Gonçalves, A.S., Kuca, K., Valis, M., LaPlante, S.R., França, T.C.C., and de Almeida, J.S.F.D., 2020, Ligand-based virtual screening, molecular docking, molecular dynamics, and MM-PBSA calculations towards the identification of potential novel ricin inhibitors, *Toxins*, 12 (12), 746.

[50] Al-Thiabat, M.G., Mohd Gazzali, A., Mohtar, N., Murugaiyah, V., Kamarulzaman, E.E., Yap, B.K., Abd Rahman, N., Othman, R., and Wahab, H.A., 2021, Conjugated β-Cyclodextrin Enhances the Affinity of Folic Acid towards FRα: Molecular Dynamics Study, *Molecules*, 26 (17), 5304.

[51] Ye, H., Wu, Q., Guo, M., Wu, K., Lv, Y., Yu, F., Liu, Y., Gao, X., Zhu, Y., Cui, L., Liang, N., Yun, T., Li, L., and Zheng, X., 2016, Growth inhibition effects of ent-11α-hydroxy-15-oxo-kaur-16-en-19-oic-acid on colorectal carcinoma cells and colon carcinoma-bearing mice, *Mol. Med. Rep.*, 13 (4), 3525–3532.

[52] Soekaryo, E., Simanjuntak, P., and Setyahadi, S., 2016, Uji Inhibisi Enzim Siklooksigenase-2 (COX-2) dari Ekstrak Daun Sirsak (*Annona muricata* Linn.) sebagai Antiinflamasi, *The 4th Univesity Research Coloquium 2016*, STIKES Muhammadiyah Pekajangan, Pekalongan, 485–492.

[53] Hashmi, M.A., Khan, A., Farooq, U., and Khan, S., 2018, Alkaloids as cyclooxygenase inhibitors in anticancer drug discovery, *Curr. Protein Pept. Sci.*, 19 (3), 292–301.

[54] Joy, M., and Chakraborty, K., 2018, Previously undisclosed bioactive sterols from corbiculid bivalve clam *Villorita cyprinoides* with anti-inflammatory and antioxidant potentials, *Steroids*, 135, 1–8.

[55] Lago, J.H.G., Toledo-Arruda, A.C., Mernak, M., Barrosa, K.H., Martins, M.A., Tibério, I.F.L.C., and Prado, C.M., 2014, Structure-activity association of flavonoids in lung diseases, *Molecules*, 19 (3), 3570–3595.